ALICE Heavy-Flavor and Jet Physics

Hadi Hassan

University of Tsukuba

15 December 2025

筑波大学
University of Tsukuba

ALICE

Flavour dependence of QCD showers

Gluon-initiated shower

Broader shower profile
Higher number of emissions

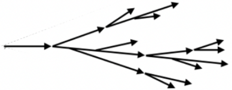

Quark-initiated shower

Narrower shower profile
Fewer emissions in the shower

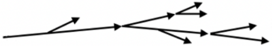

$$P_{g\to gg} = 2C_A \frac{(1-z(1-z))^2}{z(1-z)}$$

$$P_{q\to qg} = C_F \frac{1+(1-z)^2}{z}$$

Casimir colour factor:

Gluon-initiated showers are expected to have a broader and softer fragmentation profile than quark initiated showers.

$$\frac{C_A}{C_F} = \frac{9}{4}$$

Flavour dependence of QCD showers

Gluon-initiated shower

Broader shower profile
Higher number of emissions

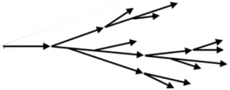

$$P_{g\to gg} = 2C_A\frac{(1-z(1-z))^2}{z(1-z)}$$

Quark-initiated shower

Narrower shower profile
Fewer emissions in the shower

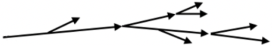

$$P_{q\to qg} = C_F\frac{1+(1-z)^2}{z}$$

Heavy-quark-initiated shower

Suppression of small angle emissions
Harder fragmentation

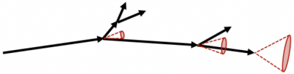

$$P_{Q\to Qg} = C_F[\frac{1}{z} - 1 + \frac{z}{2} - \frac{z(1-z)m^2}{k_\perp^2 + z^2m^2}]$$

Casimir colour factor:
Gluon-initiated showers are expected to have a broader and softer fragmentation profile than quark initiated showers.

$$\frac{C_A}{C_F} = \frac{9}{4}$$

Dead cone effect:
Heavy quarks (charm, bottom) have a larger mass, which leads to a suppression of soft emissions at small angles.

Energy-energy correlators

- QCD emissions in parton showers are angular ordered.
- Early splittings (perturbative) $\rightarrow$ wider ($R_{L,12}$)
- Late splittings (non-perturbative) $\rightarrow$ narrower ($R_{L,34}$)

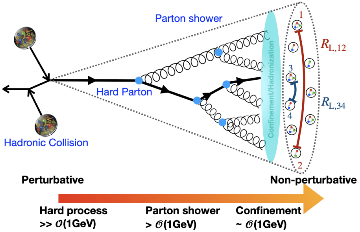

Energy-energy correlators

- QCD emissions in parton showers are angular ordered.
- Early splittings (perturbative) $\rightarrow$ wider ($R_{L,12}$)
- Late splittings (non-perturbative) $\rightarrow$ narrower ($R_{L,34}$)
- Energy-Energy Correlators (EEC) is the two-particle correlation function of the energy flow in the event:

$$\Sigma_{\mathrm{EEC}}(R_{\mathrm{L}}) = \frac{1}{N_{\mathrm{jet}}} \sum_{N_{\mathrm{jet}}} \int \sum_{i,j} \mathrm{d}R_{\mathrm{L}}' \frac{p_{\mathrm{T,i}} p_{\mathrm{T,j}}}{p_{\mathrm{T,jet}}^2} \delta(R_{\mathrm{L}}' - R_{\mathrm{L,ij}})$$

Energy weight

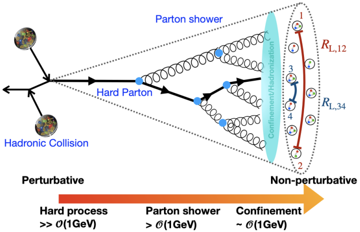

Energy-energy correlators

- QCD emissions in parton showers are angular ordered.
- Early splittings (perturbative) $\rightarrow$ wider ($R_{L,12}$)
- Late splittings (non-perturbative) $\rightarrow$ narrower ($R_{L,34}$)
- Energy-Energy Correlators (EEC) is the two-particle correlation function of the energy flow in the event:

$$\Sigma_{\mathrm{EEC}}(R_{\mathrm{L}}) = \frac{1}{N_{\mathrm{jet}}} \sum_{N_{\mathrm{jet}}} \int \sum_{i,j} \mathrm{d}R'_{\mathrm{L}} \frac{p_{\mathrm{T,i}} p_{\mathrm{T,j}}}{p^2_{\mathrm{T,jet}}} \delta(R'_{\mathrm{L}} - R_{\mathrm{L,ij}})$$

Energy weight

- EECs probes jet dynamics from perturbative (large R_L) to non-perturbative scales (small R_L).
- Energy-weighted two-particle correlation inside jet.

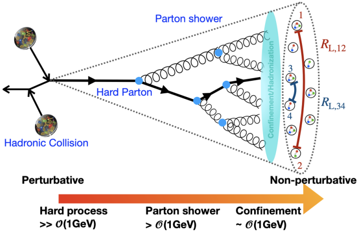

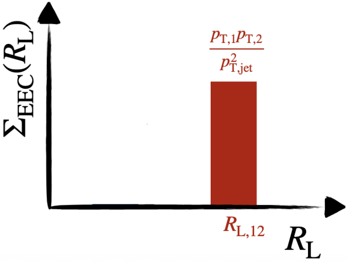

Energy-energy correlators

- QCD emissions in parton showers are angular ordered.
- Early splittings (perturbative) $\rightarrow$ wider ($R_{L,12}$)
- Late splittings (non-perturbative) $\rightarrow$ narrower ($R_{L,34}$)
- Energy-Energy Correlators (EEC) is the two-particle correlation function of the energy flow in the event:

$$\Sigma_{\mathrm{EEC}}(R_{\mathrm{L}}) = \frac{1}{N_{\mathrm{jet}}} \sum_{N_{\mathrm{jet}}} \int \sum_{i,j} \mathrm{d}R'_{\mathrm{L}} \frac{p_{\mathrm{T,i}} p_{\mathrm{T,j}}}{p^2_{\mathrm{T,jet}}} \delta(R'_{\mathrm{L}} - R_{\mathrm{L,ij}})$$

Energy weight

- EECs probes jet dynamics from perturbative (large R_L) to non-perturbative scales (small R_L).
- Energy-weighted two-particle correlation inside jet.

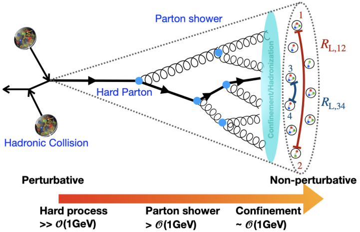

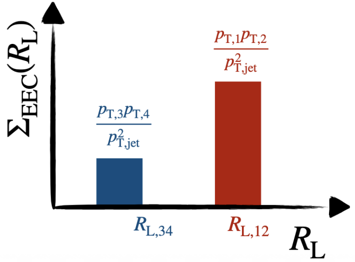

Energy-energy correlators in pp collisions

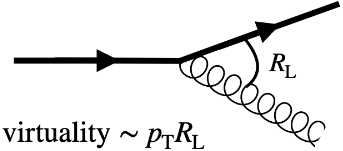

virtuality $\sim p_T R_L$

$\tau \simeq 1/(p_T R_L^2)$

arxiv:2409.12687

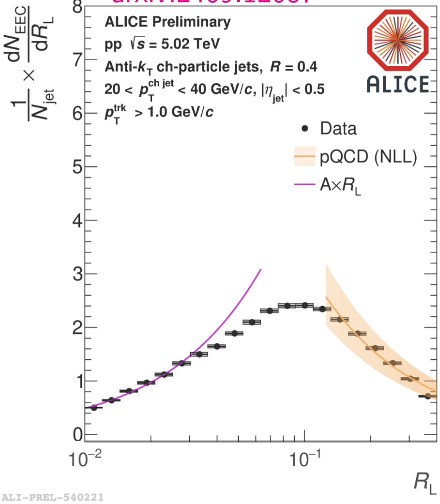

Energy-energy correlators in pp collisions

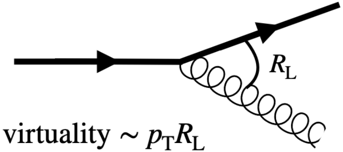

virtuality $\sim p_T R_L$

$\tau \simeq 1/(p_T R_L^2)$

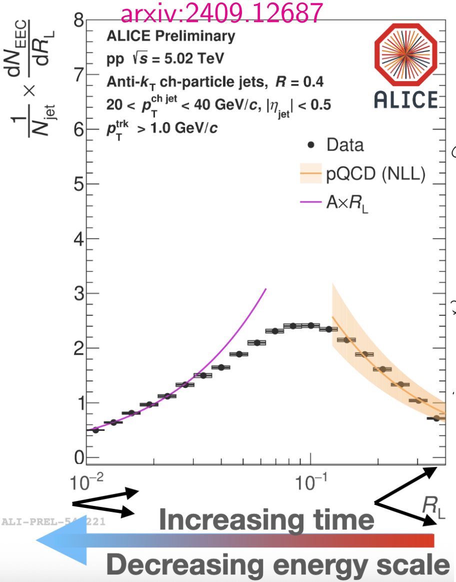

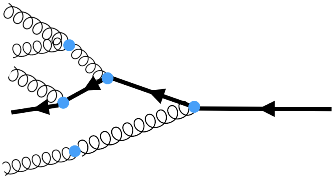

Data agrees with pQCD caclulations.

Energy-energy correlators in pp collisions

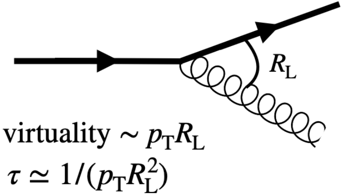

Data qualitatively follows free hadron scaling.

arxiv:2409.12687

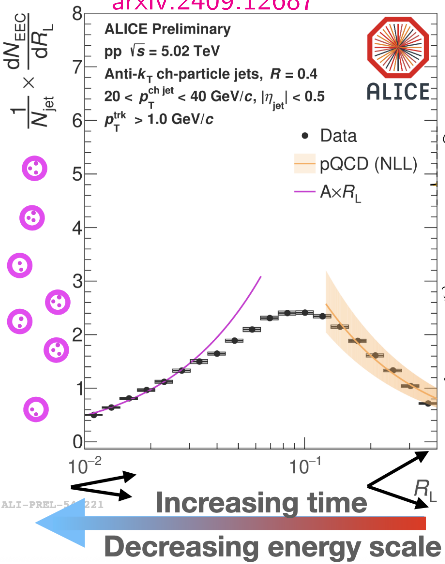

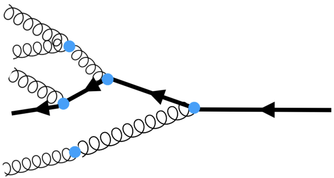

Data agrees with pQCD caclulations.

D^0-tagged jets EEC

$$\text{virtuality} \sim p_T R_L + m$$

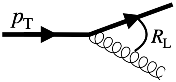

- The transition now happens at a higher virtuality scale $R_L \to m_Q/p_T$.
- Unlike light jets where the transition happens at $R_L \to \Lambda_{QCD}/p_T$.

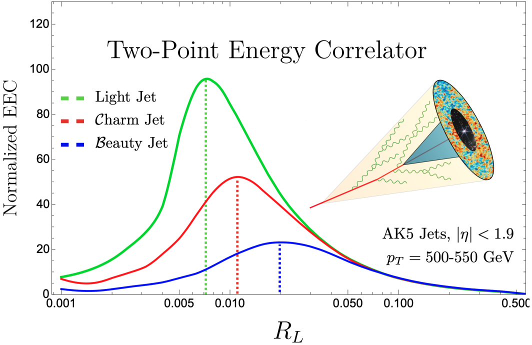

arXiv:2210.09311

D^0-tagged jets EEC

$$\text{virtuality} \sim p_T R_L + m$$

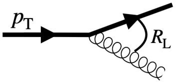

- The transition now happens at a higher virtuality scale $R_L \to m_Q/p_T$.
- Unlike light jets where the transition happens at $R_L \to \Lambda_{QCD}/p_T$.
- Ratio of HF-jet EEC to light jet shows a suppression at low R_L.
- Small angle suppression $\Rightarrow$ dead-cone effect.

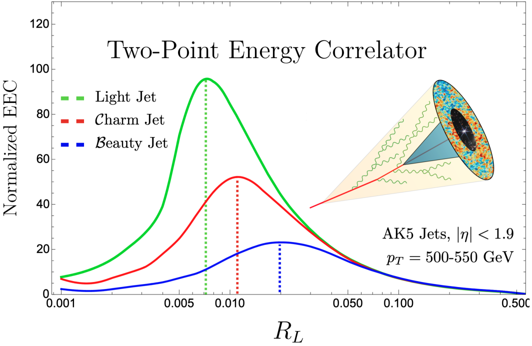

arXiv:2210.09311

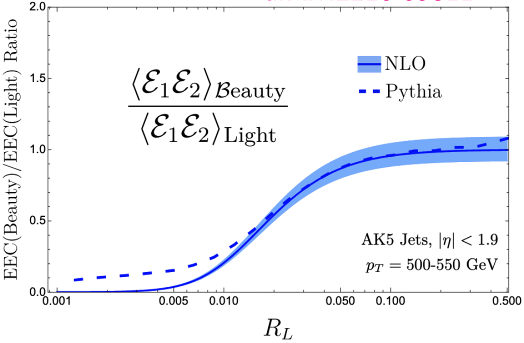

Energy-energy correlator for D^0-tagged jets

- Charm-tagged jet EECs have a lower amplitude than inclusive jet EECs $\rightarrow$ consistent with EECs for massive quarks.
- Peak position similarity of charm-tagged and inclusive jets (gluon dominated).
- Complex convolution between Casimir and mass effects in the shower and non-perturbative hadronization effects.

arxiv:2504.03431

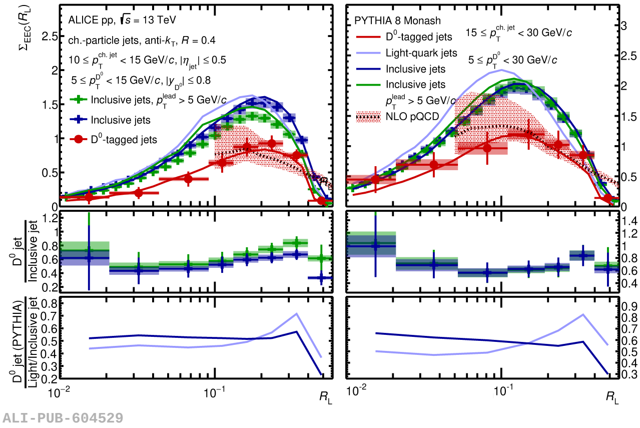

D^0-jet axes differences

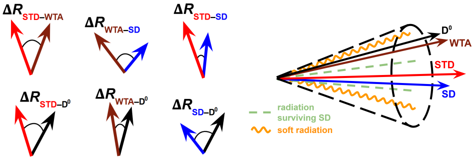

Recently published in PRD 112 (2025) 092012.

$$\Delta R_{axis} = \sqrt{(\Delta\eta)^2 + (\Delta\varphi)^2} \rightarrow \text{Opening angle between different axes}$$

Three jet axes definitions:

- Standard Jet Axis (STD): the normal jet axis obtained from the anti-ktjet clustering algorithm and E-recombination scheme.
- Winner-Take-All (WTA): the axis obtained by reclustering the jet constituents with the Cambridge/Aachen algorithm and using the WTA recombination scheme.
- Soft Drop (SD): the axis obtained by applying the Soft Drop grooming procedure to the jet and taking the axis of the resulting groomed jet.

$$\frac{\min(p_{T,1}, p_{T,2})}{p_{T,1} + p_{T,2}} > z_{cut} \left(\frac{\Delta R_{1,2}}{R}\right)^{\beta}$$

D^0-jet axes differences

Recently published in PRD 112 (2025) 092012.

$$\Delta R_{axis} = \sqrt{(\Delta\eta)^2 + (\Delta\varphi)^2} \rightarrow \text{Opening angle between different axes}$$

- WTA scheme always points to the hardest prong $\rightarrow$ D^0 meson is the winner (99% of the time is the leading particle in the hardest prong).

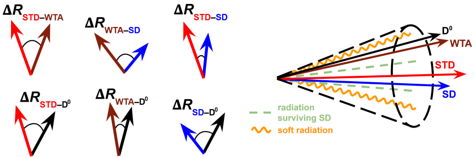

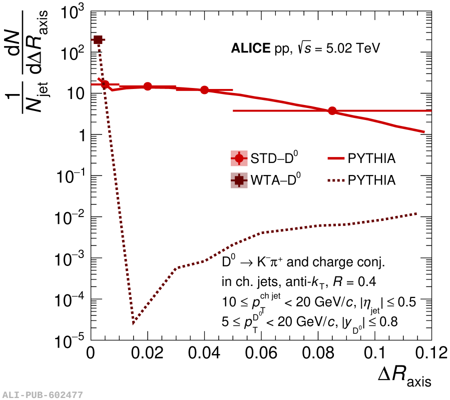

D^0-jet axes differences

Recently published in PRD 112 (2025) 092012.

$$\Delta R_{axis} = \sqrt{(\Delta\eta)^2 + (\Delta\varphi)^2} \rightarrow$$ Opening angle between different axes

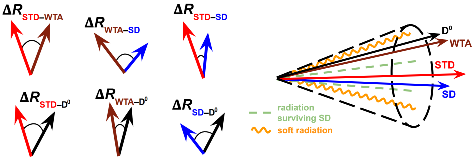

- WTA scheme always points to the hardest prong $\rightarrow$ D^0 meson is the winner (99% of the time is the leading particle in the hardest prong).
- Small ΔR region: Charm quark either emits few soft gluons or does not radiate at all.
  - STD-D^0: do not significantly tilt the jet direction w.r.t the D^0 direction.
  - SD-D^0 ($z_{cut} = 0.1$): the most grooming at small angles.
  - SD-D^0 ($z_{cut} = 0.2$): intensifying grooming further removes the jets at low ΔR.
- Large ΔR region: Charm undergoes a harder and/or wider emission

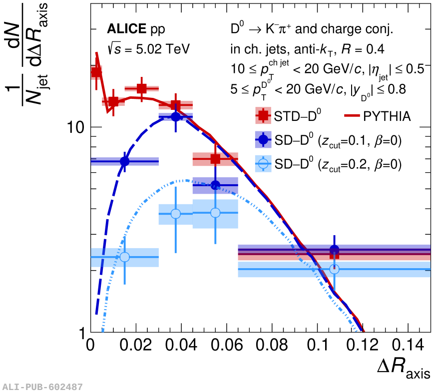

D^0 Angularities

Under IRC review.

- Observable depends on p_{T} and angular distribution of particles inside jet.
- Tuning $\alpha \to$ probe gluon vs. quark vs. heavy-quark radiation.

$$\lambda_\alpha = \sum_{i \in \mathrm{jet}} \left(\frac{p_{\mathrm{T,i}}}{p_{\mathrm{T,jet}}}\right)\left(\frac{\Delta R_{\mathrm{jet,i}}}{R_{\mathrm{jet}}}\right)^{\alpha}$$

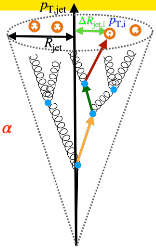

- $\alpha = 1$: sensitive to small angle radiation: Peak D^0-jets < inclusive jets with leading track cut < inclusive jets without a leading track requirement $\to$ p_{T} concentrated near the jet axis in D^0-jets, whereas it is distributed to wider angles in inclusive jets.
- $\alpha = 3$: sensitive to wide-angle radiation: the differences between the angularities of D^0-jets and inclusive jets is reduced.

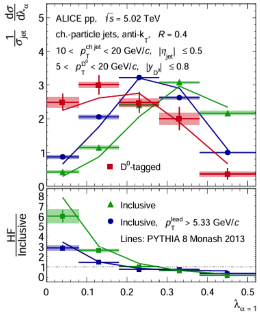

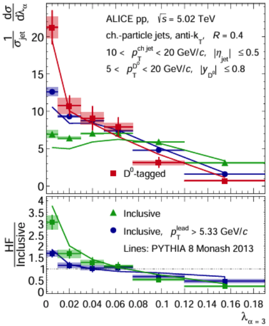

Probing the charm splitting function

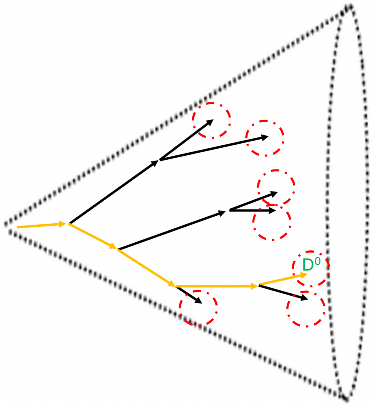

- Take advantage of angular ordering in QCD, early splittings are wider and later splittings are narrower.
- Use the Cambridge/Aachen algorithm to identify closest constituents and recluster them.
- Build up the intermediate shower.
- Grooming techniques used to remove soft splitting and keep the hard (perturbative) splitting.

$$z_g = \frac{p_{T,2}}{p_{T,1} + p_{T,2}}$$

$$\theta_g = \frac{R_g}{R} = \frac{\sqrt{\Delta\eta^2 + \Delta\varphi^2}}{R}$$

Probing the charm splitting function

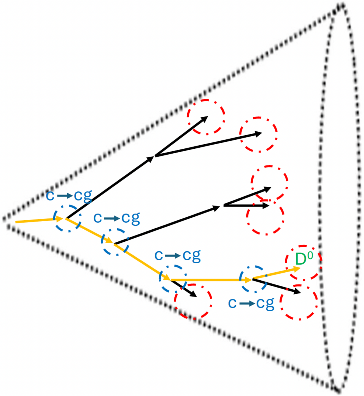

- Take advantage of angular ordering in QCD, early splittings are wider and later splittings are narrower.
- Use the Cambridge/Aachen algorithm to identify closest constituents and recluster them.
- Build up the intermediate shower.
- Grooming techniques used to remove soft splitting and keep the hard (perturbative) splitting.
- This allows us to study the splitting function.
- The presence of a heavy-flavour hadron allows us to trace the path of the charm quark through the shower.

$$z_g = \frac{p_{T,2}}{p_{T,1} + p_{T,2}}$$

$$\theta_g = \frac{R_g}{R} = \frac{\sqrt{\Delta\eta^2 + \Delta\varphi^2}}{R}$$

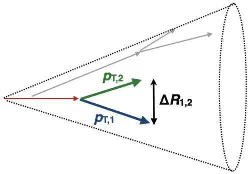

Soft Drop grooming condition:

$$z = \frac{p_{T,2}}{p_{T,1} + p_{T,2}} > z_{cut} \left(\frac{\Delta R_{1,2}}{R} \right)^{\beta}$$

$$z_{\mathrm{cut}} = 0.1, \beta = 0$$

A. J. Larkoski et al. , JHEP 1405 (2014) 146

Substructure of D^0-tagged jets

PRL 131 (2023) 192301

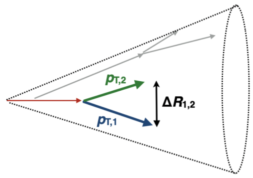

Soft Drop grooming condition:

$$z = \frac{p_{T,2}}{p_{T,1} + p_{T,2}} > z_{cut} \left(\frac{\Delta R_{1,2}}{R} \right)^{\beta}$$

$$z_{cut} = 0.1, \beta = 0$$

A. J. Larkoski et al. , JHEP 1405 (2014) 146

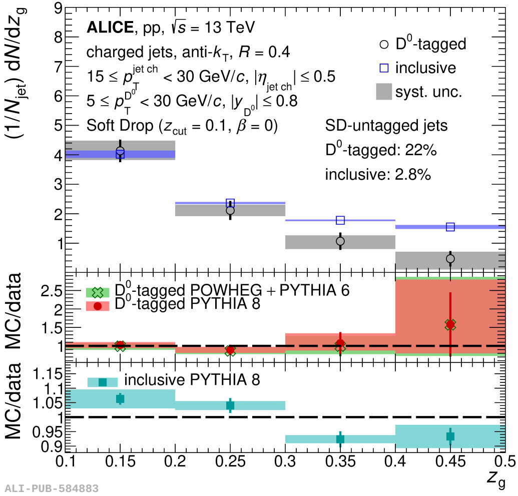

- First measurement of a flavour-enriched splitting function.
- Steeper splitting function for charm emissions as expected from mass effects.

Substructure of D^0-tagged jets

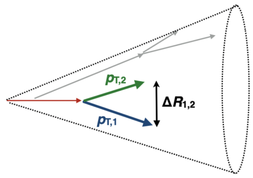

Soft Drop grooming condition:

$$z = \frac{p_{T,2}}{p_{T,1} + p_{T,2}} > z_{cut} \left(\frac{\Delta R_{1,2}}{R} \right)^{\beta}$$

$$z_{cut} = 0.1, \beta = 0$$

A. J. Larkoski et al. , JHEP 1405 (2014) 146

PRL 131 (2023) 192301

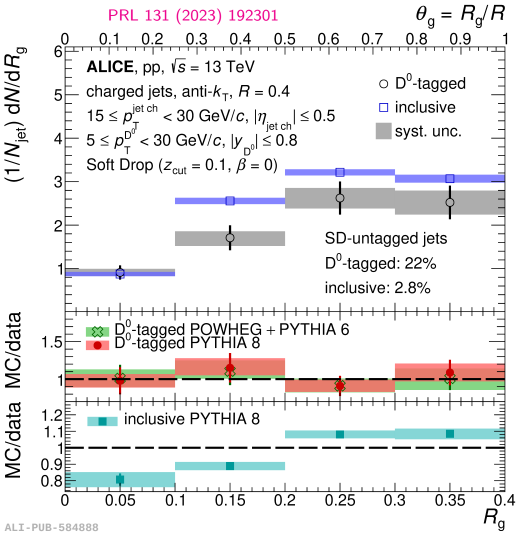

- The splitting function for charm quarks has a narrower angular distribution.
- At large angles dominated by Casimir colour effects.
- At small angles a competition between the dead cone and Casimir effects is observed.

Substructure of D^0-tagged jets

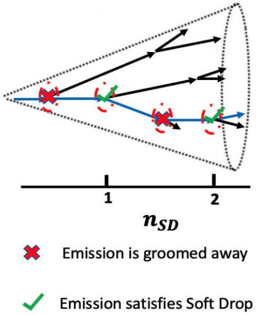

Soft Drop grooming condition:

$$z = \frac{p_{T,2}}{p_{T,1} + p_{T,2}} > z_{cut} \left(\frac{\Delta R_{1,2}}{R} \right)^{\beta}$$

$$z_{cut} = 0.1, \beta = 0$$

A. J. Larkoski et al. , JHEP 1405 (2014) 146

PRL 131 (2023) 192301

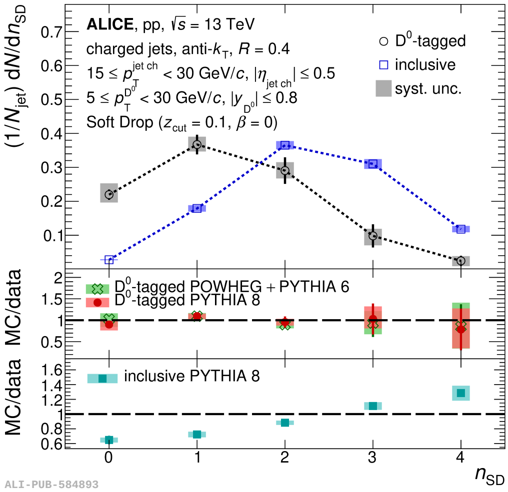

- Charm quarks emit less frequently along their evolution.

D^0-jets in Run 3 with the Upgraded ALICE Detector

- High precision measurements of flavour effects accessible.
- Boosted Decision Trees (BDT) used to tag D^0-jets.
- Finer binning, smaller uncertainty, and higher $p_{T,jet}$ reach.

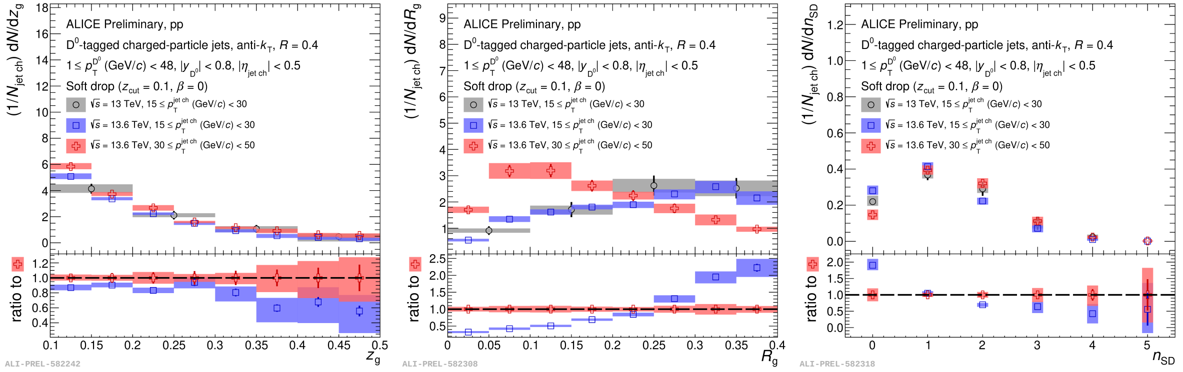

$\Lambda_c/D^0/D^\pm$ fragmentation function

- It follows the same procedure as the previous measurement.
- The upgraded detector allowed for a much better precision to measure the fragmentation function (Λ_c pT/jetpT).
- Multiplicity dependence of fragmentation function is being studied.
- Λ_c carries most of the jet energy.
- Λ_c energy fraction is smaller in HM compared to LM due to the presence of more constituents.

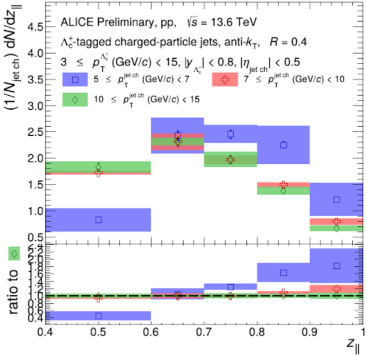

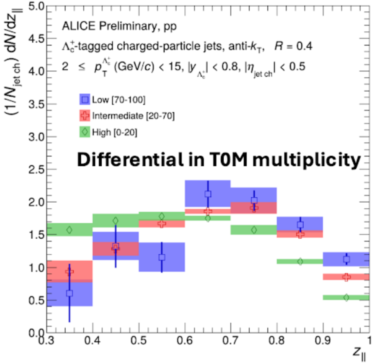

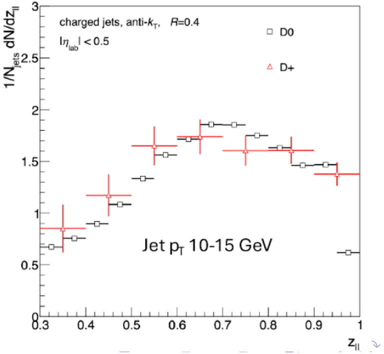

Beauty-hadron jet measurement

- First measurement of fully reconstructed beauty-hadron in pp collisions at $\sqrt{s} = 13$ TeV.
- Beauty hadrons are reconstructed via hadronic decay channels: $B^0 \to D^-\pi^+ \to \pi^-K^+\pi^-\pi^+$.
- Similar procedures as as for charm-hadron jets.
- We can measure substructure, fragmentation, and splitting function of B-jets in Run 3.

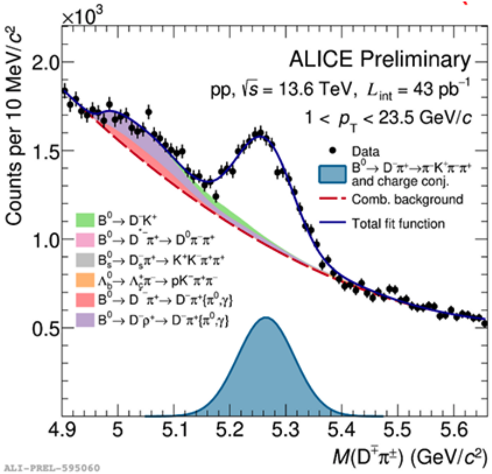

Other HF-hadron-jet measurements in Run 3

Ongoing analyses:

- D^0-jet radial profile:
  - The goal of this analysis is to investigate charm hadronization by studying the angular separation between the D^0 meson and the jet axis.
- $\Xi_c^+ \to \Xi^- \pi^+ \pi^+$ in jets.
- D_s^+ radial profile in jets.
- D^0-jet cross section in pp collisions.
- J/ψ-jet fragmentation function measurements.

Open analyses (man power needed):

- EEC in HF-jets.
- Angularities.
- Jet axes differences.
- Cross section.
- Fragmentation.
- Jet substructure.

Measurement of b-jets in pp and p-Pb collisions

ALICE JHEP, 178 (2022)

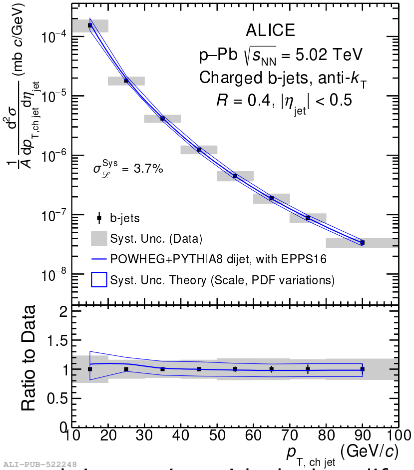

ALI-PUB-522248

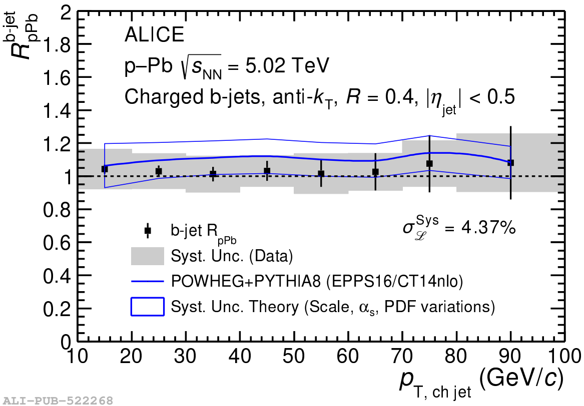

ALI-PUB-522268

- b-jet tagging with the long life time of b hadrons.
- agree with pQCD with nPDFs.

- $R_{pPb} \approx 1 \Rightarrow$ no significant cold nuclear matter effects(CNM) on b-jet production.
- Improve the precision with Run 3 to check CNM and "quenching" if any.

b-jet Tagging in Run 3 with the Upgraded ALICE Detector

- With the ALICE detector upgrade in Run 3 (notably the new ITS), b-jet tagging performance has improved.
- Traditional approaches: Impact Parameter and Secondary Vertex methods.

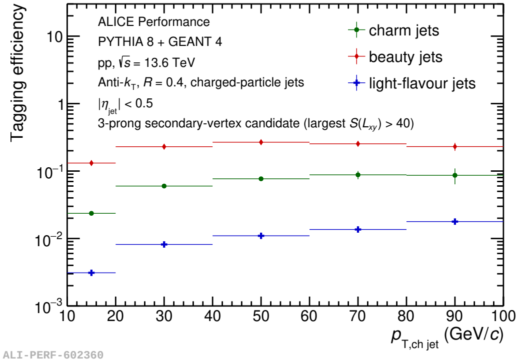

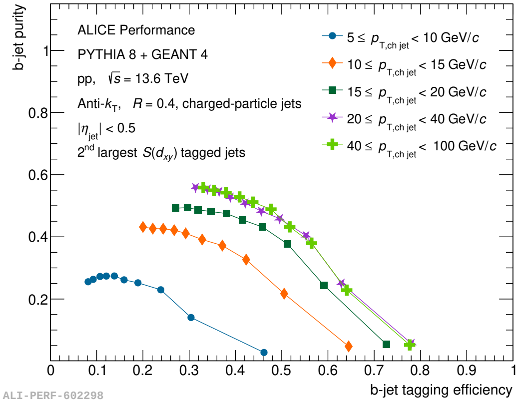

b-jet Tagging in Run 3 with the Upgraded ALICE Detector

- With the ALICE detector upgrade in Run 3 (notably the new ITS), b-jet tagging performance has improved.
- Traditional approaches: Impact Parameter and Secondary Vertex methods.
- Machine Learning approaches: Graph Neural Networks (GNNs), Convolutional Neural Networks (CNNs), and Boosted Decision Trees (BDTs).
- ML methods are train on features extracted from jets, tracks, and secondary vertices.

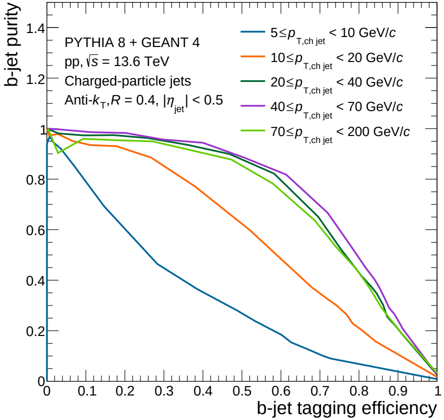

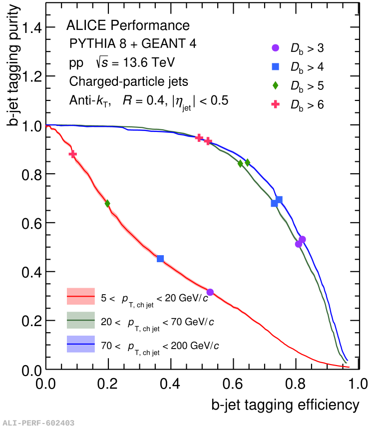

HF electron-tagged jets

- Study of substructure of HF-tagged jets via electrons.
- Based on previous HFe-jet studies, expanded to study substructure.
- Benefits: Higher statistics, well-understood ePID, and it gives access to b-jets
- Limitations: cannot reconstruct HF hadron fully which leads to the smearing of jet substructure.
- As can be seen on the figures, the substructures observable are smeared.
- Reached a consensus that the current method of tagging HF jets with electrons is not suitable for substructure studies.

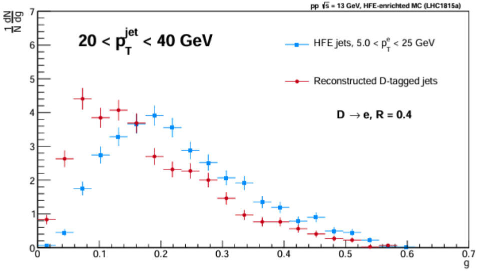

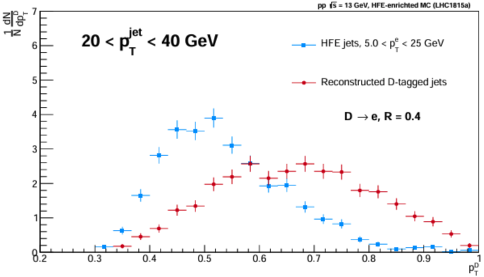

Other things that can be done with b-jets

- b-jet cross section versus multiplicity in pp collisions.
- b-jet RAA in Pb-Pb collisions.
- b-jet v2 in high multiplicity pp collisions.
- b-jet v2 in Pb-Pb collisions.
- b-jet energy flow in pp and Pb-Pb collisions.
- b-jet radial profile in pp and Pb-Pb collisions.
- di-b-jets correlations in pp and Pb-Pb collisions.
- What can we do with b-jet in light ions? What can be interesting to measure?

Summary

- Energy correlators explored to look into the transition between perturbative and non-perturbative dynamics inside jet.
- Comparison of charm-initiated and gluon-initiated jets shows significant contribution from Casimir color factor and mass effects (dead-cone effect).
- Charm mass influences the parton shower evolution of a jet.
- ML methods for b-jet tagging are being explored in Run 3.
- Studies of substructure of HF-tagged jets via electrons show that the current method is not suitable for substructure studies.
- Many other topics can be explored with HF-jets in Run 3 and beyond.

Thank you for listening

Backup

D^0-jet jet axis difference

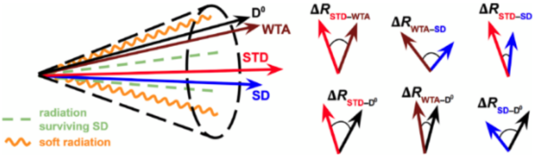

Recently published the measurement in PRD.

$$\Delta R_{axis} = \sqrt{(\Delta\eta)^2 + (\Delta\varphi)^2} \;\rightarrow$$ Opening angle between different axes

Different jet algorithm ⇔different sensitivity to gluon radiation in jet.

Least sensitive to soft radiation

Standard (Std) = clustered with anti-k_T algorithm and combine with the E-scheme

Soft Drop (groomed) (SD): Standard jet reclustered with Cambridge-Aachen with the SD condition applied to it.

$$\frac{min(p_{T_1}, p_{T_2})}{p_{T_1} + p_{T_2}} > z_{cut}\left(\frac{\Delta R_{12}}{R}\right)^{\beta}$$

Winner-Take-All axis = Standard jet reclustered with C-A algorithm and recombination with Winner-Take-All scheme (WTA) → pointing to hardest branch.

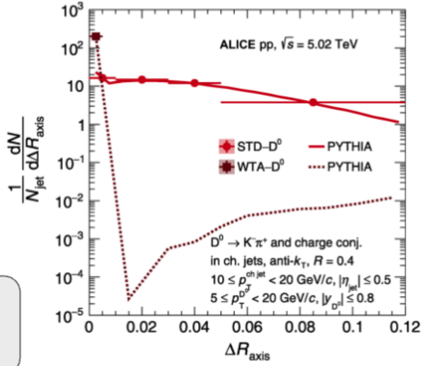

WTA axis = D^0

WTA scheme always points to the hardest prong→ D0 meson is the winner (99% of the time is the leading particle in the hardest prong). Expected due to dead-cone effect

D^0-jet jet axis difference

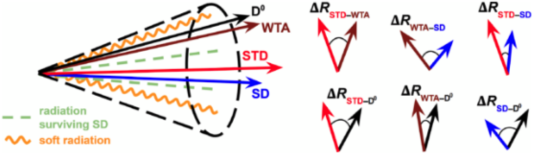

Recently published the measurement in PRD.

$\Delta R_{axis} = \sqrt{(\Delta\eta)^2 + (\Delta\varphi)^2} \rightarrow$ Opening angle between different axes

Different jet algorithm ⇔different sensitivity to gluon radiation in jet.

Least sensitive to soft radiation

Standard (Std) = clustered with anti-k_T algorithm and combine with the E-scheme

Soft Drop (groomed) (SD): Standard jet reclustered with Cambridge-Aachen with the SD condition applied to it.

$$\frac{min(p_{T_1}, p_{T_2})}{p_{T_1} + p_{T_2}} > z_{cut}\left(\frac{\Delta R_{12}}{R}\right)^{\beta}$$

Winner-Take-All axis = Standard jet reclustered with C-A algorithm and recombination with Winner-Take-All scheme (WTA) → pointing to hardest branch.

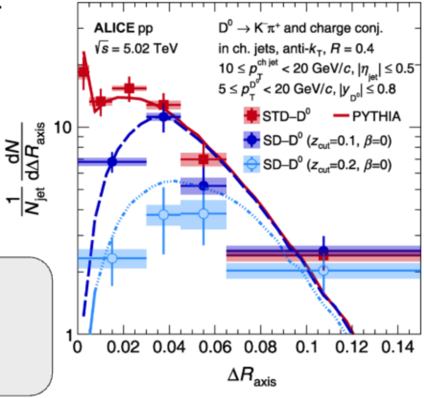

Small ΔR region: Charm quark either emits few soft gluons or does not radiate at all.

1. STD-D^0: do not significantly tilt the jet direction w.r.t the D^0 direction.
2. SD-D^0(z_{cut}=0.1): the most grooming at small angles.
3. SD-D^0(z_{cut}=0.2): intensifying grooming further removes the jets at low ΔR

Large ΔR region: Charm undergoes a harder and/or wider emission

D^0-jet angularities

Measurement under IRC review.

Observable depends on p_T and angular distribution of particles inside jet.

Tuning α → probe gluon vs. quark vs. heavy-quark radiation

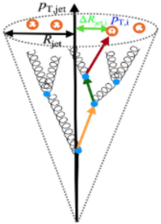

$$\lambda_\alpha = \sum_{i \in jet} \left(\frac{p_{T,i}}{p_{T,jet}} \right) \left(\frac{\Delta R_{jet,i}}{R_{jet}} \right)^\alpha$$

$$\lambda_\alpha = \sum_{i \in jet} z_i \theta_i^\alpha$$

α=1: sensitive to collinear radiation
Data: Peak **D^0-jets < inclusive jets with leading track cut < inclusive jets** without a leading track requirement.
→ p_T concentrated near the jet axis in D^0-jets, whereas it is distributed to wider angles in inclusive jets.

α=3: sensitive to wide-angle radiation
Date: the differences between the angularities of D^0-jets and inclusive jets is reduced.

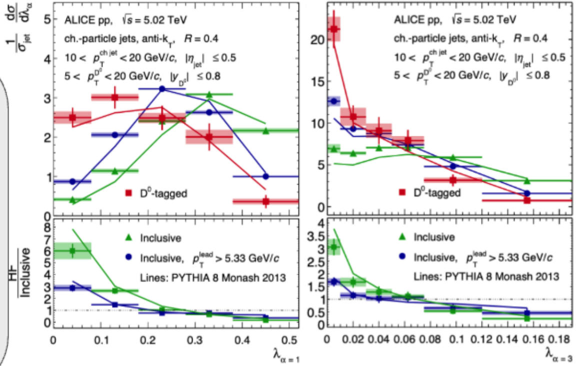

Beauty-Jet R_{AA}

- Beauty-jet R_{AA} for different jet Rs and different centralities.

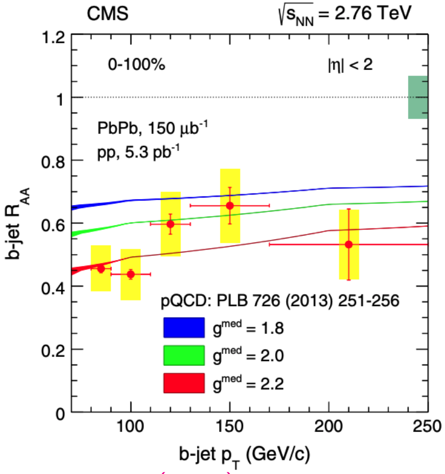

PRL 113, 132301 (2014)

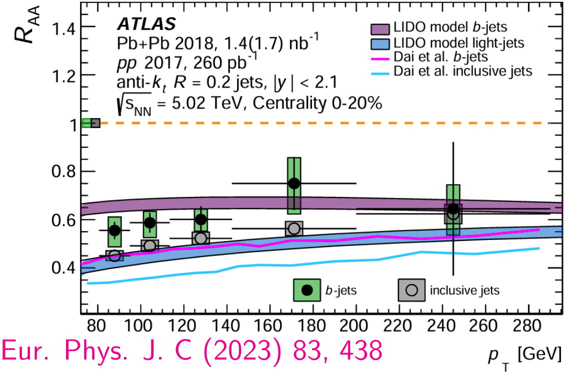

Eur. Phys. J. C (2023) 83, 438

Multiplicity dependence

- Multiplicity dependent b-jet production (already started).
- Many multiplicity bins and many different b-jet Rs.

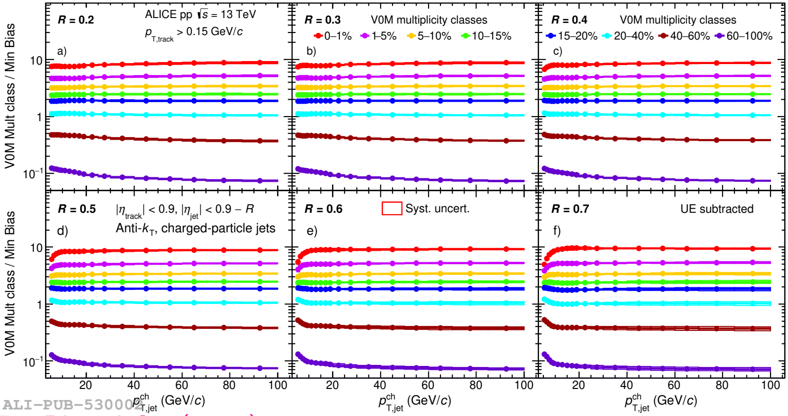

Eur.Phys.J.C82(2022)6,514

Energy flow inside jets

- Studying the energy flow inside the jets.
- The jets are reconstructed with different Rs and then geometrically matched.
- The momentum difference is studied for the same jet with different Rs.
- For inclusive jets it showed the energy is largely contained around the jet axis.

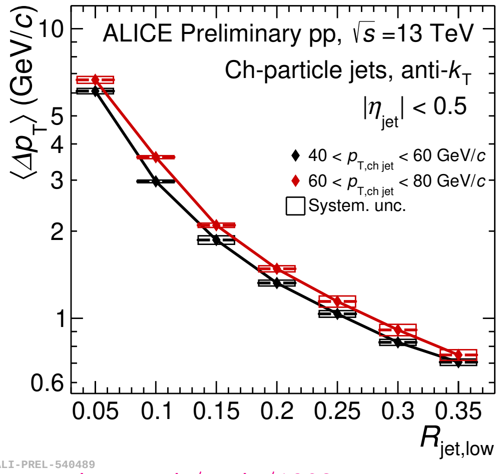

alice-notes.web.cern.ch/node/1302

Jet shapes

- The transverse momentum profile of charged particles in the jets is defined as:

$$P(\Delta r) = \frac{1}{\Delta r_b - \Delta r_a}\frac{1}{N_{jet}}\Sigma_{jets}\Sigma_{trk\in(\Delta r_a,\Delta r_b)} p_T^{trk},$$

- This profile is normalized to unity within the measured range of $\Delta R < 1$ to produce the jet shape:

$$\rho(\Delta r) = \frac{P(\Delta r)}{\Sigma_{jets}\Sigma_{trk\in(\Delta r<1)} p_T^{trk}},$$

- A redistribution of the energy in b jets to larger distances from the jet axis is observed in Pb-Pb collision.
- This medium-induced redistribution is larger for b jets than for inclusive jets.

Phys. Lett. B 844 (2023) 137849

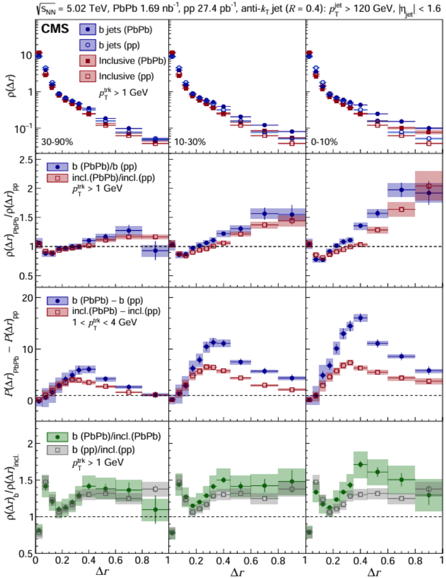

Di-b jets

- Select two back-to-back jets within $|\Delta\phi| > \frac{2\pi}{3}$
- Apply the tagger on the two hardest jets in the events.
- Calculate the pT balance x_J between these two jets and compare between pp and PbPb collisions.
- b-jets have a larger imbalance in the most central PbPb collisions due jet quenching effect.
- The imbalance of b-dijets is comparable to that of inclusive dijets.

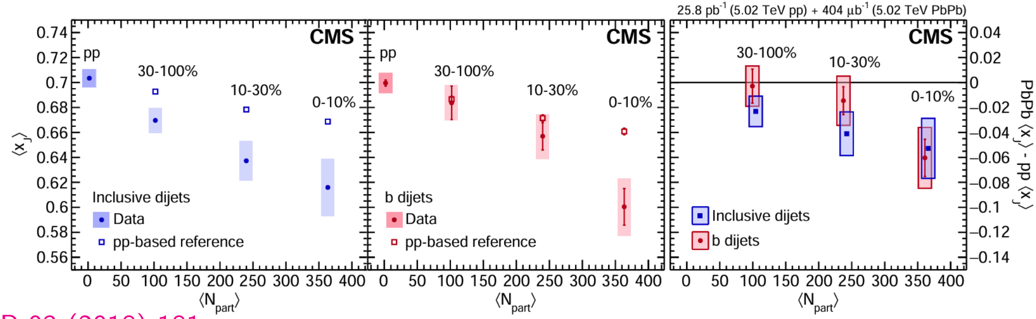

JHEP 03 (2018) 181